Available online at www.eccomasproceedia.org
Eccomas Proceedia COMPDYN (2025) 3023-3031

ECCOMAS
Proceedia

COMPDYN 2025
10th ECCOMAS Thematic Conference on
Computational Methods in Structural Dynamics and Earthquake Engineering
M. Papadrakakis, M. Fragiadakis (eds.)
Rhodes Island, Greece, 15-18 June 2025

BEARING RESISTANCE OF HINGED THIN-WALLED PROFILES

F. Morelli[1], D. Mattoccia[1], A. Natali[1]

[1]Department of Civil and Industrial Engineering, University of Pisa. Largo Lucio Lazzarino 2, 56122, Pisa, Italy.

e-mail: francesco.morelli@unipi.it, daniele.mattoccia@phd.unipi.it, agnese.natali@unipi.it

Abstract

Thin-walled elements are widely adopted for many structural solutions, especially for the one characterised by high element repetition and the necessity of quick assembly. The extensive use of such elements, also in more challenging design situations, implies the need for increasingly more performing elements, both in terms of resistance and ductility, especially in relation to seismic applications. In this framework, this paper presents an experimental campaign on hinged thin-walled elements that could be adopted as diagonal profiles (subjected to axial tensile-compression forces) for trellis structures. Being such low-thickness profiles, the driving design parameter for the element may be the bearing resistance of the bolted connection, which value is strongly affected by many geometrical parameters (thickness of the component, distance of the connection hole from the end section), in addition to the strength of the material. The experimental campaign investigates the bearing resistance of thin-walled elements with varying positions of the connection hole to evaluate how geometrical parameters affect bearing resistance and failure modes. Bearing resistance under compression load is also tested, and an inner empty hole is added to assess possible strategies to control its value. Numerical models reproducing the experimental behavior are made to replicate and better understand the observed failure modes and possible correlation to the geometrical parameters.

Keywords: Cold-formed thin-walled elements, Experimental behaviour, Numerical calibration, Bearing resistance.

ISSN:2623-3347 © 2025 The Authors. Published by Eccomas Proceedia.
Peer-review under responsibility of the organizing committee of COMPDYN 2025.
doi: 10.7712/120125.12630.25357

1 INTRODUCTION, RESEARCH OBJECTIVES AND METHODOLOGY

Thin walled elements are widely used in the construction market to realise structures as lightweight residential buildings, light-weight partitions and industrial steel racks [1, 2]. In the last case, in particular, the thin-walled elements are subjected to high internal forces, making the design challenging due to the strong sensitivity of such elements to phenomena such as buckling and plastic ovalisation [3–5]. Increasing the latter can be highly challenging when coupled with a capacity design approach that requires the connection to be overstrength compared to the connected elements. Indeed, the simplest way to increase the bearing resistance consists in incrementing the thickness of the connected profiles or the strength of the steel. Anyway, both these solutions lead to an enhancement of the elements' resistance, nullifying the efforts in the framework of the capacity design. Another possibility is to increase the number of bolts or their diameter. However, this solution is often not feasible due to the limited available space for the connection, meaning that using a higher number of bolts or larger diameters would require larger elements, which would again result in the same issues mentioned above.

To address this issue, some studies have been performed, aiming at allowing seismic-resistance or dissipation also in the case of structures with thin walled elements. One developed strategy is based on protecting the connection of the dissipative element through the reduction of its cross-section [6–8]. As an alternative, the present paper examines the potential of utilising and controlling plastic ovalisation as a localised mechanism to improve the overall seismic performance. To control the bearing resistance related to the plastic ovalisation, the strategy proposed in [9] and validated in [10, 11] is applied, in which the distance of the bolt from the free end of the profile or a blot-less hole is varied to calibrate the bearing resistance respectively associated to tensile or compression force in the element. To this end, an experimental campaign is first carried out, varying these distances and assessing the actual bearing resistance. Then, numerical simulations are performed and calibrated based on the experimental results. The calibration process highlighted the most influential modelling parameters on the different aspects of plastic ovalisation (strength, stiffness, ductility) and helped in better understanding the possible mechanisms associated with bearing resistance. Moreover, the calibrated models will enable the extension, in future research, of evaluating bearing resistance to different configurations, allowing the development of analytical formulas or mechanical models.

2 EXPERIMENTAL CAMPAIGN

The experimental campaign aimed at evaluating the bearing resistance of a cold formed profile provided with two holes, see Figure 1b-c. The external hole is used to allocate the bolt, and its distance *e1* from the free end is varied to study its influence on the bearing resistance of the profile subjected to tension. The internal hole is blot-less and is used only as a mean of calibration of the bearing resistance of the profile subjected to compression. It is expected that low distance from the two holes, *p1*, leads to low bearing resistance, while a high value makes the bolt-less hole irrelevant. To this end, 10 specimens were subjected to axial loading with variable values of e1 and p1, as shown in Table 1.

Specimen ID	e1 [mm]	p1 [mm]	Specimen ID	e1 [mm]	p1 [mm]
T1	16	39	C1	29	20
T2	23		C2		29
T3	29		C3		39
T4	36		C4		44

T5	44	C5	49

Table 1: position of the holes in the specimens.

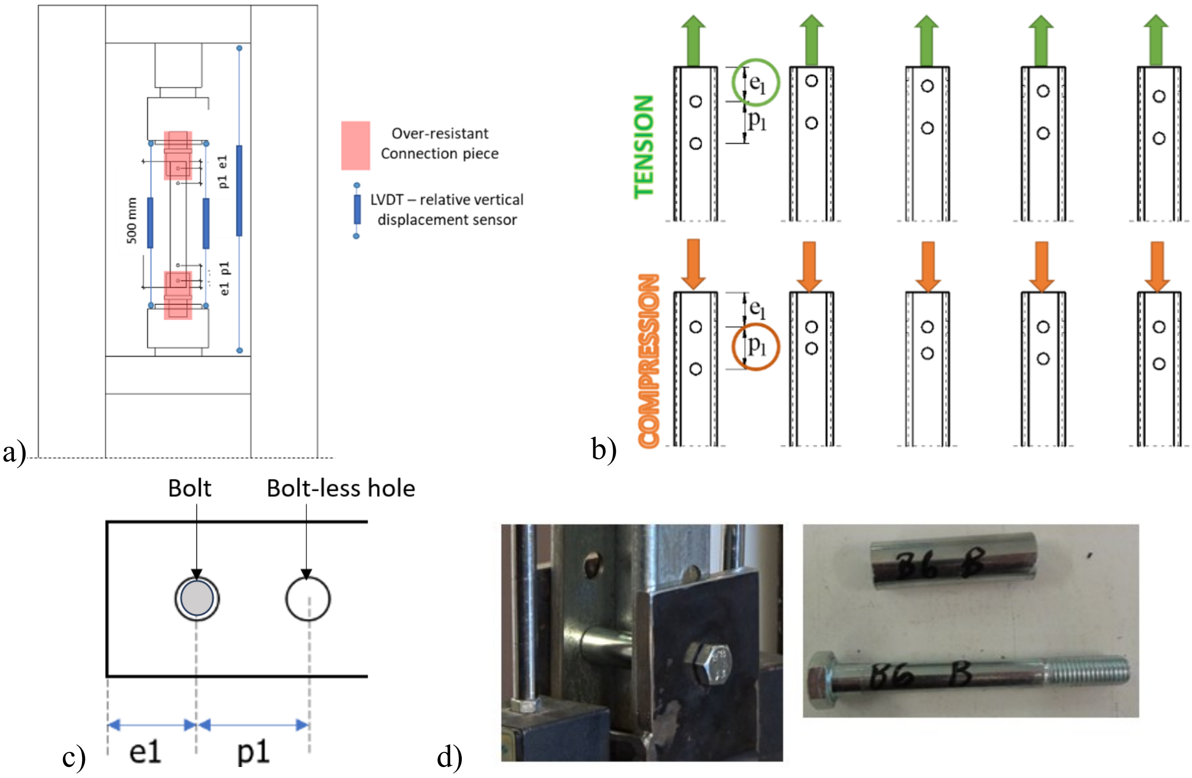

a) b) c) d)

Figure 1: Test setup for the uniaxial test, a) global view, b) layout of the holes' position in the specimens and c) position of the bolt and the bolt-less hole.

The specimens were connected to the universal testing machine through a couple of stiff plates and a single bolt, see Figure 1d). The bolt is provided with a hollow cylinder to avoid excessive distortion of the profile panels. Figure 2 shows the results of the tensile test for the specimens T1 to T5 in terms of force-displacement. It can be seen that for high values of *e1* (specimens T3, T4 and T5), the behaviour is practically constant, meaning that if the bolt is placed far enough from the free edge, the bearing resistance and the stress distribution is not influenced by the free edge. On the contrary, the behaviour of specimens T1 and T2 is quite different from the others and to small values of *e1* correspond to low values of resistance and ductility. All these results are in quite good agreement with the design rules adopted by international standards (e.g., Eurocodes). Figure 3 shows similar results for the compression tests: Also in this case, when the distance from the bolt-less hole is "high enough", the behaviour doesn't change when increasing *p1* further. The only case tested in which the influence of the bolt-less hole is evident is the C5 case with a *p1* of 20mm. In this case, the bolt-less hole influences the distribution of plastic stress associated with the bearing mechanism, resulting in a lower global bearing resistance.

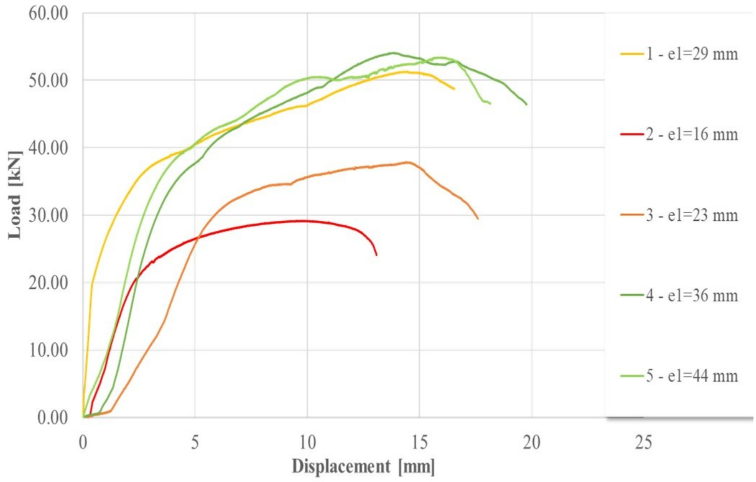

Figure 2: Results of the tensile test varying the distance from the free edge e_1.

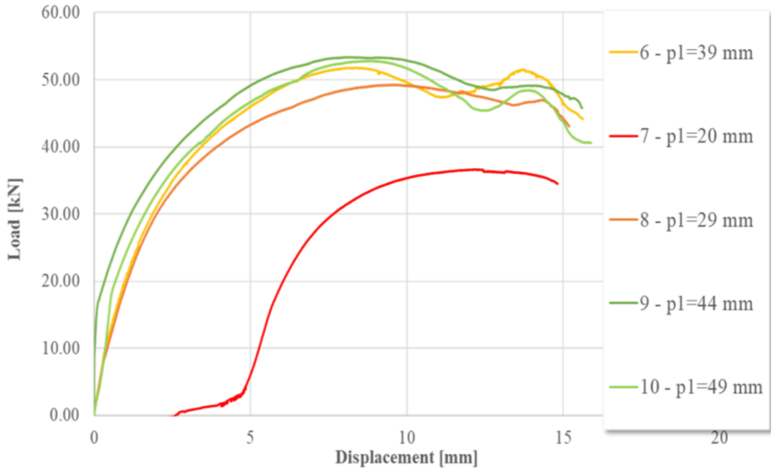

Figure 3: Results of the compression test varying the distance among the bolted and boltless hole p_1.

3 NUMERICAL SIMULATION

To provide a better understanding of the experimental results, a finite element (FE) model of the whole test setup was developed in Abaqus. To take into account all possible elements influencing the force-displacement behaviour, the connecting plates and the bolt were also modelled. The mesh size was decreased in the contact zones, where the highest concentration of stresses was expected, as shown in Figure 4. To consider also the effects of the internal hollow cylinder, an internal constraint that prevents the inward movement of the profile holes' edges was applied as schematically shown in Figure 5b.

Two types of models were investigated: in the first, the profile is represented through shell elements, while in the second, it is represented through solid elements. The following paragraph describes the modelling approach and the main results obtained from the numerical simulations.

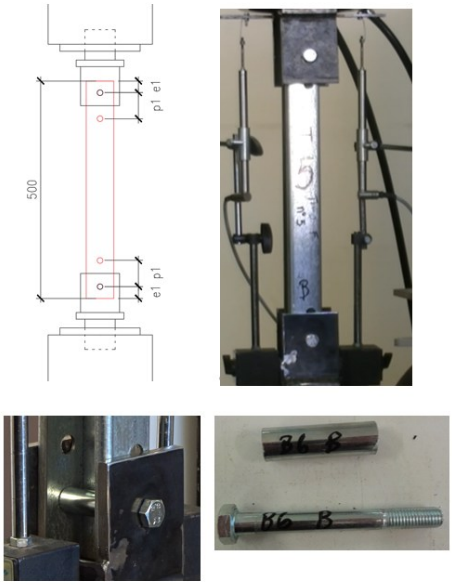

a)

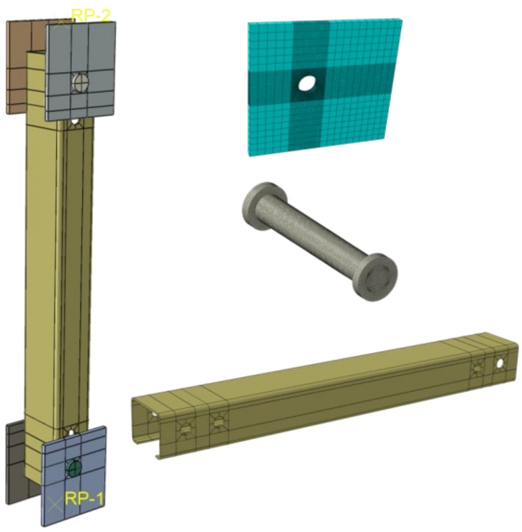

b)

Figure 4: Comparison between the a) global test setup and b) global model view.

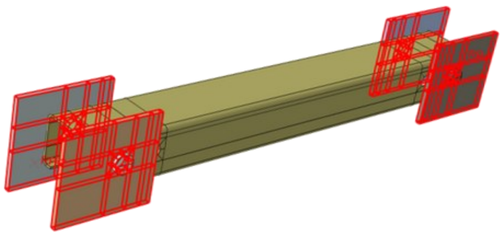

a)

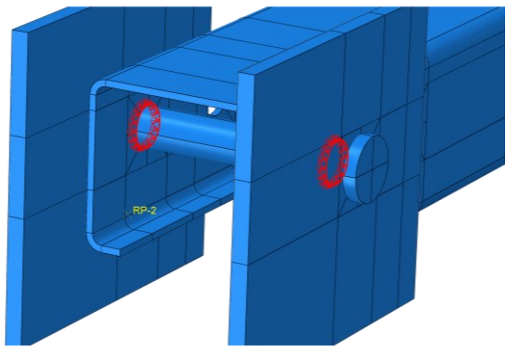

b)

Figure 5: Modeling of the a) connection plates and b) internal constraints.

3.1 Shell FE model

In the shell FE model, the whole cold-formed profile was represented through a shell model with a more refined mesh in the zone around the hole, where higher stresses were expected (see Figure 6a). The bolt was modelled as a rigid element. Figures 6c-d show the distribution of equivalent Von Mises stresses due to the bolt-profile contact with the typical formation of a plastic zone around the hole. Figure 7 shows the experimental (blue line) and numerical (black line) force-displacement curves for specimen T3 (in tension). The model is quite capable of representing the initial stiffness of the system and its maximum strength. Still, the post-elastic behaviour shows a significant discrepancy, and the numerical model is unable to capture the softening effects, mainly due to the local distortion of the profile. Initial attempts to replicate experimental behaviour were made using simplified shell models. Initially, the bolt was represented via a multipoint constraint (MPC), which proved inadequate, as it did not capture the evolution of contact between the bolt and the hole. This aspect plays a critical role in the bearing failure mechanism. A second shell model was developed using a rigid cylindrical surface to simulate the bolt, allowing for localised Hertzian contact pressures to develop around the hole. While this configuration better reproduced the stress distribution and out-of-plane deformation observed experimentally, it still failed to capture the necessary material accumulation and plastic flow around the bolt hole. As a result, the shell model significantly underestimated the connection's ductility, with the numerical force-displacement response reaching collapse after only 4 mm of displacement compared to 15 mm in the experimental test.

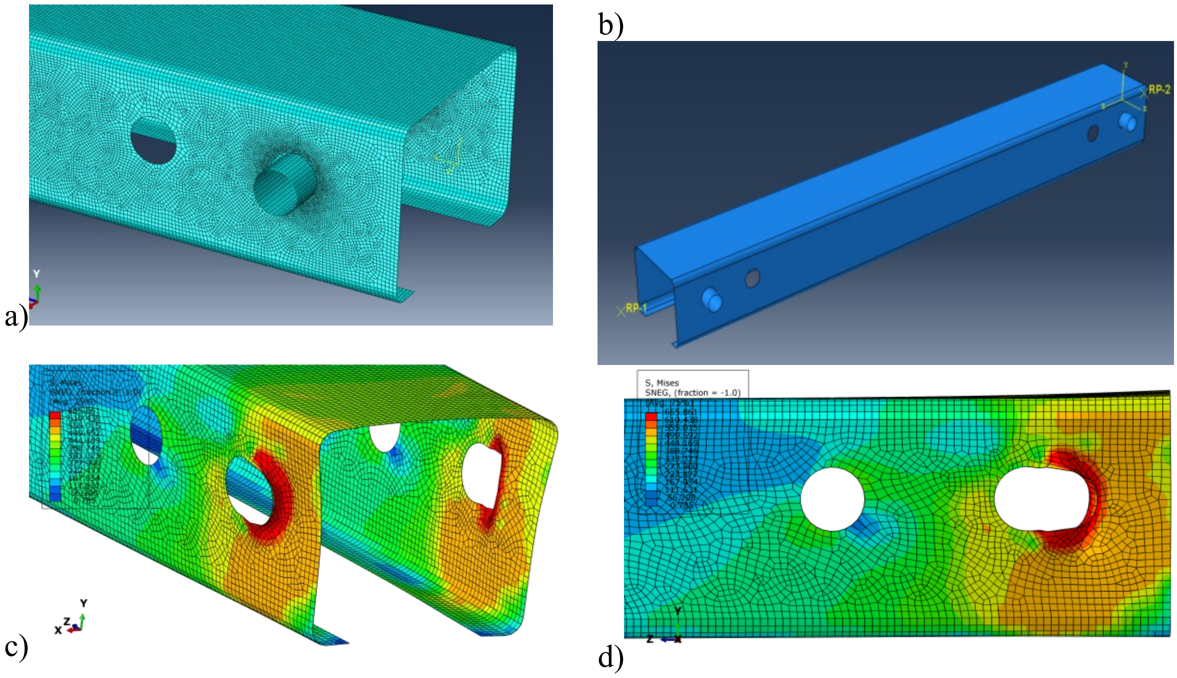

Figure 6: Shell FE model: a-b) global view and c-d) distribution o stresses in case of tensile test.

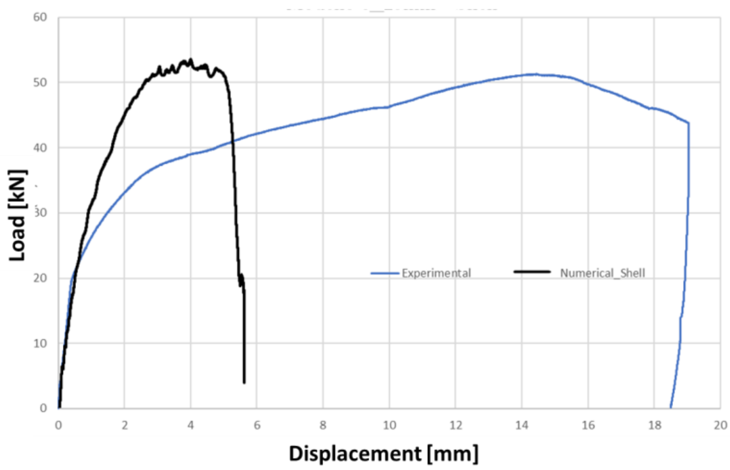

Figure 7: Experimental (blue line) and shell FE model numerical (black line) force-displacement curve for the tensile test.

3.2 Solid FE model

To overcome the limits shown by the shell FE model, a solid model of the profile, with three elements in the thickness direction, was studied. The first solid model did not consider any initial imperfections and his geometry, similarly to the shell FE model, represented the nominal profile geometry. The mesh has the same organisation of the shell model with more elements in the bolt-profile contact zone. Figure 8 shows the results of the numerical analysis in terms of local stresses and deformation (figure 8a) and of force-displacement curve (figure 8b). It is evident that the solid model is capable of better representing the post-elastic behaviour with increased ductility; however, in this case, the drop in resistance occurs earlier than the experimental evidence suggests.

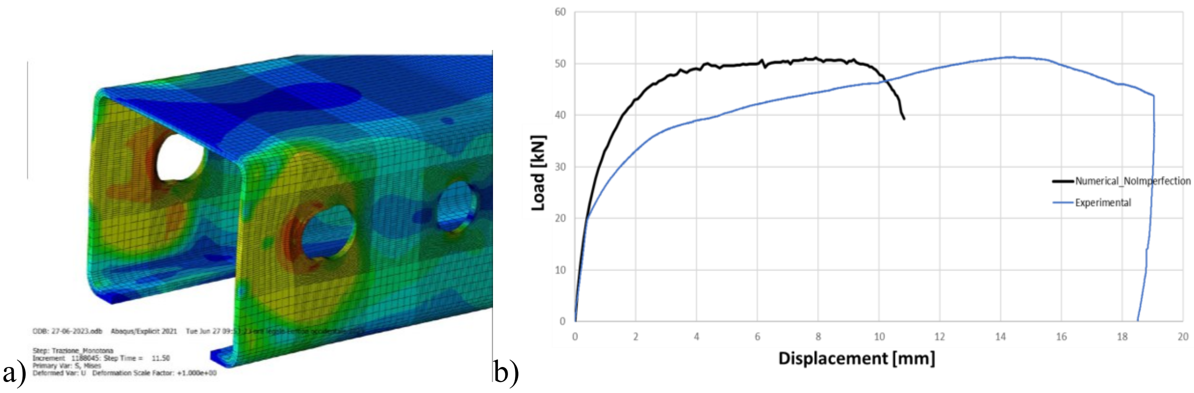

Figure 8: Experimental (blue line) and solid FE model, without initial imperfections, numerical (black line) force-displacement curve for the tensile test.

Several aspects of the numerical modelling were studied to understand the possibility of catching the complete ductility of the connection related to the bearing resistance. The most influential one of them resulted from the local imperfections around the hole, mainly due to the realisation of the hole itself. To this end, a local imperfection was introduced, and the analysis was carried out again, resulting in the final hole configuration and force-displacement curves shown in Figures 9 and 10 for both the tensile and compression tests. The presence of the imperfection "guides" the hole's edge into the effective deformation, increasing the ductility of the system to a value very close to the one assessed experimentally.

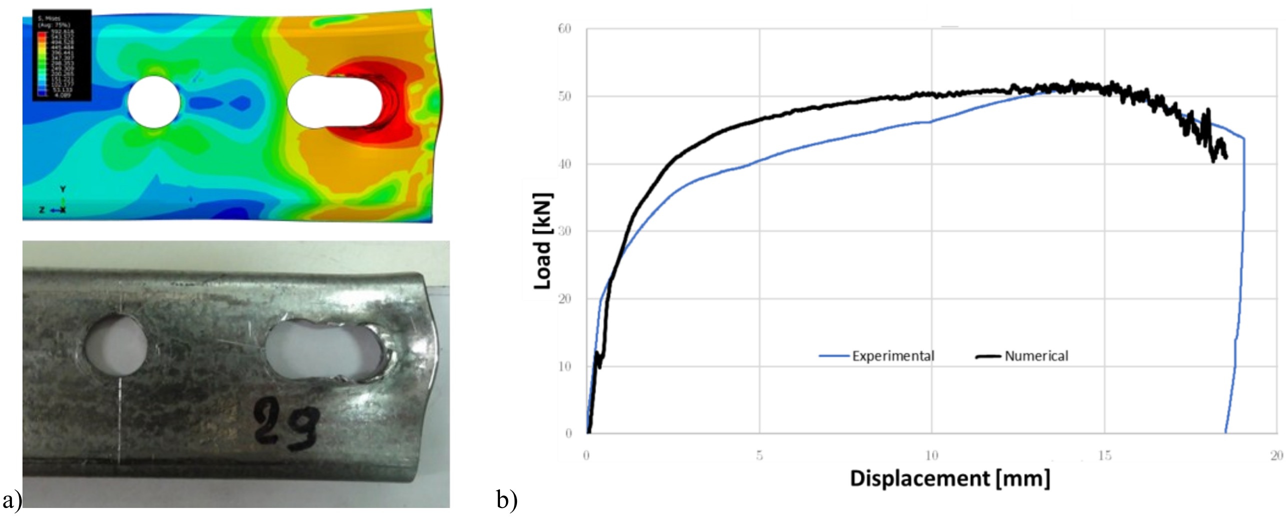

Figure 9: Tensile tests: comparison of the experimental and numerical a) status of the specimen at the end of the test and b) force-displacement curve (experimental is the blue line, numerical the black one).

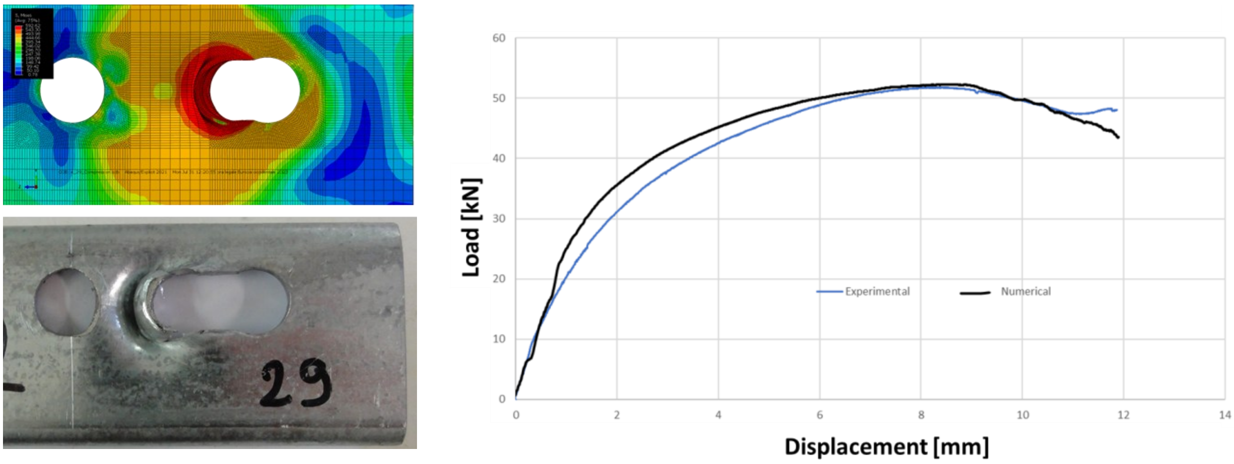

Figure 10: Compression tests: comparison of the experimental and numerical a) status of the specimen at the end of the test and b) force-displacement curve (experimental is the blue line, numerical the black one).

4 CONCLUSIONS

This study explored the bearing resistance of cold-formed thin-walled steel profiles with bolted hinged connections through both experimental testing and detailed numerical simulations. The research focused on evaluating the possibility of harnessing controlled local deformation at the bolt hole to improve connection ductility and ensure a reliable failure mechanism in seismic applications.

The experimental campaign investigated the influence of geometric parameters on connection performance, specifically the edge distance (*e1*) in tension and the spacing between holes (*p1*) in compression. The results revealed a consistent behavioural trend: when *e1* and *p1* are sufficiently large, the bearing resistance stabilises and is primarily governed by the material properties and profile thickness. Conversely, small values of these parameters lead to early failure, lower resistance, and reduced ductility due to localised instabilities and tearing.

Finite element models developed in Abaqus successfully reproduced the observed experimental behaviour, particularly when incorporating solid elements and accounting for geometric imperfections around the bolt holes. These imperfections proved essential to replicating the ductile response and deformation modes. While shell models were effective in capturing the initial stiffness and peak strength, they were insufficient to describe the post-peak softening response and the full plastic development of the connection.

Overall, the findings confirm the viability of the strategy as an effective method for achieving controlled and ductile failure in bolted thin-walled connections. By concentrating deformation in predefined regions, this approach allows for a predictable and resilient seismic response. The numerical framework established here lays the groundwork for further parametric studies and supports the future development of simplified yet accurate design tools for thin-walled steel structures used in seismic applications, such as automated rack-supported warehouses. Further studies are still needed to understand the effective influence of the local imperfections and to measure them experimentally.

REFERENCES

[1] Tsarpalis D. “Ductile Seismic Design, Performance Assessment, and Taxonomic Characterization of Steel Racking Systems”, Doctoral Thesis, National Technical University of Athens, Institute of Steel Structures.

[2] Tsarpalis D, Vamvatsikos D, Delladonna F, et al. Macro-characteristics and taxonomy of steel racking systems for seismic vulnerability assessment. *Bull Earthquake Eng* 2022; 20: 2695–2718.

[3] Kondratenko A, Kanyilmaz A, Castiglioni CA, et al. Structural performance of automated multi-depth shuttle warehouses (AMSWs) under low-to-moderate seismic actions. *Bull Earthquake Eng*. Epub ahead of print 26 October 2021. DOI: 10.1007/s10518-021-01193-y.

[4] Natali A, Morelli F, Salvatore W. Seismic performance of currently designed Automated Rack Supported Warehouses. *7h World Congress on Civil, Structural, and Environmental Engineering (CSEE’22)*.

[5] Natali A, Morelli F, Salvatore W. On the Seismic Design and Behavior of Automated Rack Supported Warehouse. *Bulletin of Earthquake Engineering*, 2022, DOI: 10.21203/rs.3.rs-1577721/v1 (2022, accessed 11 July 2022).

[6] Natali A, Morelli F. Seismic performance of dissipative automated rack supported warehouses. In: *8th European Congress on Computational Methods in Applied Sciences and Engineering*. CIMNE. Epub ahead of print 2022. DOI: 10.23967/eccomas.2022.241.

[7] Natali A, Morelli F. Experimental validation of dissipative reduced-section thin walled diagonals for seismic-resistant Automated Rack Supported Warehouses. *Procedia Structural Integrity* 2023; 44: 2334–2341.

[8] Natali A, Morelli F, Salvatore W. Rack Supported Warehouses with reduced-section diagonals for improved dissipative seismic behaviour. *Journal of Constructional Steel Research*.

[9] Tsarpalis D, Vamvatsikos D, Natali A, et al. A ductile seismic design strategy for the cross-aisle direction of racking systems. *Bull Earthquake Eng* 2024; 22: 4083–4113.

[10] Natali A, Morelli F, Salvatore W, et al. Experimental validation of plastic ovalization strategy for seismic- resistant Automated Rack Supported Warehouses.

[11] Natali A, Morelli F, Vulcu C, et al. Experimental behaviour of ductile diagonal connections for rack supported warehouses. *Bull Earthquake Eng*. Epub ahead of print 28 August 2024. DOI: 10.1007/s10518-024-01999-6.